Osmotic regulation of Rab-mediated organelle docking

Christopher L. Brett and **Alexey J. Merz**[*]
Department of Biochemistry, University of Washington, Seattle WA 98195-7350

SUMMARY

Osmotic gradients across organelle and plasma membranes modulate the rates of membrane fission and fusion; sufficiently large gradients can cause membrane rupture [1–6]. Hypotonic gradients applied to living yeast cells trigger prompt (within seconds) swelling and fusion of *Saccharomyces cerevisiae* vacuoles, while hypertonic gradients cause vacuoles to fragment on a slower time scale [7–11]. Here, we analyze the influence of osmotic strength on homotypic fusion of isolated yeast vacuoles. Consistent with previously reported *in vivo* results, we find that decreases in osmolyte concentration increase the rate and extent of vacuole fusion *in vitro*, while increases in osmolyte concentration prevent fusion. Unexpectedly, our results reveal that osmolytes regulate fusion by inhibiting early, Rab-dependent docking or predocking events, not late events. Our experiments reveal an organelle-autonomous pathway that may control organelle surface to volume ratio, size and copy number: decreasing the osmolyte concentration in the cytoplasmic compartment accelerates Rab-mediated docking and fusion. Fusion, by altering the organelle surface-to-enclosed volume relationship, in turn reduces the risk of membrane rupture.

Keywords

Mechanosensation; SNARE; G protein; Rab-GAP; Yck3p; casein kinase

RESULTS

Organelle-autonomous regulation of fusion by osmolyte concentration

The yeast vacuole is, like the mammalian lysosome, the terminal compartment of the endocytic pathway. Our cell-free fusion system (Fig. S1) places purified yeast vacuoles in a standard reaction buffer containing approximately physiological salts, 200 mM sorbitol, and ATP. Decreasing the sorbitol concentration in the buffer increased the extent (Fig. 1A) and rate (Fig. 1B) of fusion. Conversely, increasing the sorbitol concentration decreased the extent and rate of fusion, and lengthened the lag time prior to fusion (Fig. 1B). Quantitative morphometry (Fig. 1C) of fusion reactions corroborated the results from content mixing assays. These *in vitro* results closely mirror observations of living cells [7–11]. The inhibitory effect of sorbitol is due to osmotic strength rather than sorbitol's specific physical or chemical properties. Replacement of sorbitol with other small polar osmolytes including trehalose, glycerol, or sucrose (Fig. S2A; unpublished data) yielded results comparable to sorbitol. Glycerol and trehalose are present at up to several % (wt/vol) in living yeast cells [12], indicating that they

---

*For correspondence: merza@u.washington.edu, http://faculty.washington.edu/merza/, Tel: +1 206 616-8308.

are not intrinsic inhibitors of membrane traffic. Dissolved solutes alter viscosity and, through excluded volume and hydration effects, the chemical activity of water [13,14]. 15% dextran-5 is more viscous than 15% sorbitol but has <1/10th as much osmotic strength; it slightly stimulated fusion (Fig. S2A). Thus viscosity *per se* does not prevent fusion. The results obtained with dextran-5 and bovine serum albumin (Fig. S2A) further indicate that excluded volume effects [13,14] cannot explain inhibition by sorbitol. Excluded volume and hydration effects also shift the ionic optima of many enzymatic reactions. Fusion is most efficient at ~125 mM [KCl]; this sharp ionic optimum did not shift appreciably as the sorbitol concentration was varied (Fig. S2B). Thus, small polar solutes decrease the rate of fusion by increasing osmotic strength. This effect is organelle-autonomous, requiring neither cytosol nor an intact plasma membrane.

Osmotic control of an early docking or pre-docking subreaction

To map the osmotic effect to specific subreactions of fusion (Fig. S1), we performed kinetic studies using stage-specific inhibitors (Fig. 2A). A master fusion reaction was initiated. At intervals, reaction aliquots were transferred to tubes containing the specified treatments, incubated further, and assayed for fusion. This approach tracks loss of susceptibility to each treatment, *i.e.*, the kinetics of completion of each subreaction. Treatments that modulate only early subreactions exhibit kinetics shifted left of the anti-Vam3 (docking) curve. Treatments that modulate later subreactions map between the anti-Vam3 and "ice" (content-mixing) curves. Unexpectedly, 1.4 M sorbitol inhibited fusion at early but not late time points (Fig. 2A). After 20 minutes, fusion was >90% resistant to sorbitol addition, even though docking (anti-Vam3 curve) was <80% complete and content mixing ("ice" curve) was only ~30% complete. Lowering sorbitol to 100 mM yielded identical kinetics: fusion was accelerated at early but not late times.

Because the osmitic effect mapped to early docking, we hypothesized that osmolytes modulate the kinetics of early- or intermediate-stage subreactions. To test this hypothesis, subreaction kinetics were assayed at three sorbitol concentrations (Fig. 2B). The earliest subreaction, Sec18/17-mediated priming [15,16], was not substantially influenced by osmotic strength. Sec17 release from the membrane, a biochemical correlate of priming, was also unaltered (Fig. 2B, inset). All subsequent stages of the reaction were accelerated by reduced sorbitol concentration (100 *vs.* 200 mM sorbitol), and slowed as sorbitol was added: tethering and docking (rGdi1, an inhibitor of Rab GTPases); *trans*-SNARE complex formation (anti-Vam3); and content mixing (MARCKS effector domain peptide; MED [17]). Thus, osmolytes regulate early docking and change the kinetics of Rab-mediated subreactions. We next asked whether osmolytes regulate tethering, operationally defined by the formation of clusters of associated vacuoles [9,18]. Consistent with the kinetic and staging data, increasing buffer osmolarity strongly decreased the efficiency of tethering (Fig. 2C).

Osmolytes functionally destabilize Ypt7:GTP and the HOPS complex

To further evaluate the molecular basis of the link between osmotic strength and fusion, dosage sensitivities for several fusion inhibitors were measured at four sorbitol concentrations (Fig. 3 and Fig. S3). Osmolyte did not systematically change the IC$_{50}$ (50% inhibitory concentration) for affinity-purified antibodies raised against the priming factor Sec17 (Fig. S3A and Fig. 3C) or against the SNARE Vam3 (Figs. 3A and 3C). Unaltered IC$_{50}$ values were also obtained for MED peptide [17], a late stage inhibitor of fusion that chelates acidic phospholipids (Fig. S3B). In contrast, dose-response relationships for two Rab-specific inhibitors, the Rab-chelating chaperone rGdi1 and the GAP (GTPase activating protein) rGyp1$_{TBC}$, were closely linked to osmotic strength. IC$_{50}$ values for rGdi1 and rGyp1$_{TBC}$ increased by nearly an order of magnitude as osmolyte was decreased (Fig. 3C; compare 3A to 3B). Consistent with this result, *in vivo* overproduction of a second Ypt7 GAP, Gyp7, caused superinhibition of vacuole fusion

by osmolyte, both in intact cells and in cell-free assays (Brett *et al*., submitted). Thus, osmolytes inhibit Rab-regulated subreactions of fusion.

The Ypt7 effector complex HOPS is anchored to the membrane by active Ypt7:GTP, so membrane association of HOPS provides a functional proxy for Ypt7 activation [19,20]. Differential centrifugation experiments revealed that HOPS subunits were stabilized on membranes at low osmotic strength, but dissociated into the supernatant as osmotic strength was increased (Fig. 4A). Additional experiments with the Rab chaperone rGdi, and experiments with the poorly-hydrolyzable GTP analog GTPγS (which stabilizes activated Ypt7) further support this interpretation (Brett *et al*., submitted). Taken together, the data indicate that osmolytes functionally and biochemically destabilize Ypt7:GTP and its HOPS effector complex.

Rab hyperactivation or bypass partially reverses osmotic effects

We asked if treatments that increase the quantity of active Rab GTPase, or attenuate the Rab requirement, could restore fusion at elevated osmotic strength. First, we exploited our previous finding that the recombinant SNARE rVam7 bypasses the priming requirement for Sec18/17, and ATP [21,22]. rVam7 also reduces the Rab requirement and stabilizes HOPS on the vacuole membrane [21–24]. At elevated sorbitol concentrations, rVam7 restored fusion to about half the level observed under the standard condition (Fig. 4B, top). At lower sorbitol concentrations (100 mM), rVam7 slightly suppressed fusion. This effect might result from SNARE-mediated lysis [24].

Second, we tested whether osmolyte-mediated inhibition is attenuated when there is more active Rab on the vacuole membrane. Gyp7 is the major Ypt7 GAP *in vivo*, and vacuoles purified from *gyp7Δ* cells have elevated levels of both Ypt7:GTP and HOPS (Brett *et al*., submitted). When fusion of vacuoles from *gyp7Δ* cells was measured at different concentrations of osmolyte, the effect of osmolyte was attenuated, as with rVam7 addition (Fig. 4B, middle). Moreover, addition of rVam7 to vacuoles isolated from *gyp7Δ* cells had an additive effect, resulting in fusion at elevated osmotic strength that approached the standard condition (not shown).

Third, we exploited the finding that removal of the vacuolar casein kinase I Yck3 dramatically reduces the requirement for Ypt7:GTP both *in vitro* [11] and *in vivo* (Brett *et al*., submitted). Vacuoles isolated from *yck3Δ* mutant cells (Fig. 4B, bottom), like vacuoles from *gyp7Δ* mutants, fused more robustly than vacuoles from wild type cells as the osmolyte concentration increased. Hence the inhibitory effect of osmotic strength is attenuated by three independent manipulations that either stabilize the activated Rab or decrease the Rab requirement.

DISCUSSION

Osmoregulation of docking and fusion is widespread, but the mechanisms of osmotic sensing and the molecular targets of regulation are unknown. In *Paramecium*, membrane tension generated by osmotic pressure was hypothesized to trigger cycles of vacuole exocytosis for locomotion [2]. In mammalian cells the rapid coalescence of intracellular organelles, triggered by hypoosmotic gradients, was reported almost a century ago [1]. There is a general correlation between low osmolarity in the cytoplasm, or high osmolarity in an extracytoplasmic compartment, and fusion [3–6]. For example, exocytosis is triggered by extracytoplasmic osmolytes such as sucrose [5,6], and inhibited by osmolyte in the cytoplasmic compartment [3]. Our data reveal that osmotic shifts influence fusion when applied during early docking, but are without effect during later subreactions. Our results reveal that osmolytes can control an organelle's docking machinery in an organelle-autonomous manner, and are fully consistent with earlier *in vivo* observations [7–11], .

In principle, osmosensors could operate directly, *e.g.*, by detecting changes in hydration, or indirectly, by sensing changes in membrane properties as osmotic gradients cause water and ionic species to flow across a membrane. Dai *et al.* recorded spontaneous lateral tension changes of ~40 µN/m during exocytosis and endocytosis in RBL cells [4]. Both organelle:organelle and exocytotic fusion events introduce slack into the product membrane, increasing the organelle's or cell's volume. This in turn increases the capacity for inward water movement without lysis. Thus, the ability of the docking machinery to respond to osmolytes may serve to prevent membrane tension from rising to perilous (lytic) levels during osmotic stress. Lytic tension for lysosomes and vacuoles may be lower than for other membranes, as lysis might be accelerated by lipases and other hydrolases that reside within the organelle lumen. Hypoosmotic stress can rupture lysosomes, to catastrophic effect [25], and experiments by Starai and coworkers [24] indicate that SNARE overabundance promotes membrane rupture, indicating that even normal membrane traffic functions are not without hazards. Coupling of the docking machinery to cytoplasmic osmolyte concentration or to transmembrane osmotic gradients may be central to maintenance of organelle surface-to-volume relationships and membrane integrity.

EXPERIMENTAL PROCEDURES

Yeast Strains

For fusion assays, we used complimentary strain pairs of either BJ3505 (*MATα pep4*::*HIS3 prb1-1.6R his3–200 lys2–801 trp1101* (*gal3*) *ura3–52 gal2 can1*) and DKY6281 (*MATα leu2– 3 leu 2–112 ura3–52 his3-200 trp1-901 lys2–801*) or BY4742 *pho8Δ* and BY4742 *pep4Δ* (*MAT α ura3Δ leu2Δ his3Δ lys2Δ pep4Δ*::*neo*; Invitrogen Corp., Carlsbad, CA). BJ3505 *gyp7Δ::URA3* and DKY6281 *gyp7Δ*::*URA3* were gifts from Dr. Dieter Gallwitz (Max-Planck-Institute of Biophysical Chemistry, Göttingen, Germany). BY4742 *yck3Δ pho8Δ* (=AMY809) and BY4742 *yck3Δ pep4Δ* (=AMY807) were constructed by crossing and sporulating BY4741 *yck3Δ* (*MATa his3Δ leu2Δ met15Δ ura3Δ yck3Δ*::*neo*; Invitrogen Corp.) against BY4742 pep4Δ::*neo* or BY4742 pho8Δ::*neo*. Genotypes of the resulting haploid strains were confirmed by PCR and DNA sequencing.

Reagents

All biochemical reagents were purchased from Sigma-Aldrich Corp. (St. Louis, MI) or Invitrogen Corp., except as indicated, and were of biotechnology grade or better. The endoglucanase fraction of Zymolyase 20T (Seikigaku) was purified by cation exchange chromatography before use in vacuole isolation. Purified proteins used include: recombinant Vam7 (rVam7; [21] and M. Schwartz and AJM, submitted); recombinant Gdi1 (rGdi1) purified from bacterial cells using a CBP-intein fusion system provided by V. Starai and W. Wickner; recombinant catalytic domain of Rab-GAP Gyp1p (rGyp1$_{TBC}$)[19], synthetic MARCKS Effector Domain peptide [17]; and recombinant protease inhibitor Pbi2. Rabbit polyclonal sera raised against Vps41, Vps33, Vps18, Vps11, Ypt7, Sec17 and Vam3 were gifts from W. Wickner (Dartmouth College, Hanover, NH), and were affinity purified and in some cases cross-adsorbed against cell lysates from corresponding yeast deletion mutants to eliminate cross-reactivity. The protein reagents used in fusion assays were prepared in 10 mM Pipes-KOH, pH 6.8, 200 mM sorbitol (PS), or were exchanged into this buffer by dialysis or size exclusion chromatography.

Fusion

Vacuoles were purified according to Haas *et al.* (1995). Isolated vacuoles (6 µg) were incubated for 90 min. at 27°C in standard reaction buffer: PS buffer supplemented with salts (0.5 mM MgCl$_2$, 125 mM KCl), CoA (10 mM), Pbi2 (with or without ATP-regenerating system (0.5 mM ATP, 0.1 mg/ml creatine kinase, 40 mM creatine phosphate). Vacuoles were always added

last to a premixed reaction cocktail, unless otherwise specified. Bypass fusion was initiated with recombinant Vam7 (100 nM, except as indicated). Osmotic gradients were imposed by reducing or adding sorbitol to the standard fusion reaction buffer (200 mM sorbitol). Like sorbitol, KCl concentrations were adjusted without compensatory equiosmolar changes in other buffer constituents. The solution total osmolalities (Fig. 1A) were measured using a Vapro 5520 vapor pressure osmometer (Wescor Inc., Logan, UT). As indicated, reactions also contained rGdi1p, rGyp1$_{TBC}$, anti-Sec17p antibody, anti-Vam3 antibody, rGyp1$_{TBC}$, MED, or GTPγS. Total volume of each fusion reaction was 30 µl. Fusion reactions were prepared using BY4742 $pho8\Delta$ (or DKY6128; alkaline phosphatase deficient) and $pep4\Delta$ (or BJ3505; protease deficient) vacuoles (3 µg each) with or without genomic deletion of $YCK3$ ($yck3\Delta$) or GYP7 ($gyp7\Delta$). Homotypic vacuole fusion was measured using a biochemical complementation assay ([26]; see [18] for quantitative characterization of the reporter system). Fusion (content mixing) was quantified by measuring the ALP-catalyzed evolution of p-nitrophenolate at 400 nm. Signals were then subtracted from a background control reaction either lacking ATP or incubated on ice; the signal-to background ratio under our standard conditions routinely exceeds 25:1. Results are reported relative to signals obtained under standard fusion conditions (200 mM sorbitol with ATP), unless otherwise indicated. Under standard conditions the mean extent of fusion was 3.5 (n = 98) fusion units as defined previously, corresponding to about two rounds of fusion [18,26]. In addition, we verified that sorbitol does not alter the efficiency of ALP activation in assays with vacuole lysates (data not shown) [18]. Vacuole membrane release of Sec17, Ypt7p and HOPS components was determined with fusion reactions containing only protease-deficient vacuoles (6 µg $pep4\Delta$ or BJ3505). After incubation at 27°C for 10, 40 or 70 min., fusion reactions were immediately sedimented by centrifugation at $20,000 \times$ g for 5 min. at 4°C. Pellet and supernatent fractions were fractionated by SDS-PAGE and analyzed by immunoblotting.

Microscopy

To examine vacuole morphology $in\ vitro$, $pep4\Delta$ vacuoles were incubated for times indicated (30 or 70 min.) at 27°C in fusion reaction buffer containing 3.0 µM FM4-64. After incubation, reactions were placed on ice, 2 µl of each reaction was then mixed with 0.4% agarose, mounted on a chilled glass coverslip and immediately imaged. Vacuole diameters and contact zone lengths were measured from micrographs subjected to high-pass and sharpening filters using Image/J v. 1.36b software (Wayne Rasband, NIH, Wachington, DC). Vacuole clustering analysis was performed as in Mayer and Wickner (1997) with minor modifications: no cytosol was added to reactions, and KCl was not reduced to 40 mM. In brief, 5 µg of $pep4\Delta$ vacuoles were incubated at 27°C for 30 min. in reaction buffer containing MgCl$_2$ (1 mM) and 3.0 µM FM4-64 in the absence or presence of a lower than conventional concentration of ATP-regenerating system (0.3 mM ATP). 2 µl of the reaction was then imaged as above. Micrographs were acquired using an Olympus IX71 light microscope system outfitted with an EMCCD (Andor iXon), ultrabright green and blue light-emitting diodes (> 350 n,mW output) synchronized with the camera by custom electronics, a PlanApoN 1.45 NA 60x objective lens and AndorIq v. 6.0.3.62 software (Andor Bioimaging, Nottingham, UK). Micrographs were processed using Image/J v. 1.36b (J. Rasband, U.S. National Institutes of Health, http://rsb.info.nih.gov/ij/) and PhotoshopCS v. 8.0 (Adobe Systems, Inc.) software.

Data Analysis

Where applicable, datasets were fit to sigmoidal dose-response functions using a nonlinear least-squares algorithm. log IC$_{50}$ values were extracted from the sigmoidal fits using Prism v. 4.0c software (GraphPad, San Diego, CA). Data are reported as mean ± s.e.m. Statistical comparisons were performed using two-tailed Student's t tests (paired or unpaired, as appropriate); significance was assumed at the 5% level, after Dunn-Sîdak compensation for repeated comparisons.

Supplementary Material

Refer to Web version on PubMed Central for supplementary material.

Acknowledgments

REFERENCES

1. Hogue MJ. The effect of hypotonic and hypertonic solutions on fibroblasts of the embryonic chick heart in vitro. J Exp Med 1919;30:617–648. [PubMed: 19868382]

2. Tominaga T, Allen RD, Naitoh Y. Cyclic changes in the tension of the contractile vacuole complex membrane control its exocytotic cycle. J Exp Biol 1998;201:2647–2658. [PubMed: 9716516]

3. Zimmerberg J, Sardet C, Epel D. Exocytosis of sea urchin egg cortical vesicles in vitro is retarded by hyperosmotic sucrose: kinetics of fusion monitored by quantitative light-scattering microscopy. J Cell Biol 1985;101:2398–2410. [PubMed: 4066763]

4. Dai J, Ting-Beall HP, Sheetz MP. The secretion-coupled endocytosis correlates with membrane tension changes in RBL 2H3 cells. J Gen Physiol 1997;110:1–10. [PubMed: 9234166]

5. Fatt P, Katz B. Spontaneous subthreshold activity at motor nerve endings. J Physiol 1952;117:109–128. [PubMed: 14946732]

6. Bekkers JM, Stevens CF. NMDA and non-NMDA receptors are co-localized at individual excitatory synapses in cultured rat hippocampus. Nature 1989;341:230–233. [PubMed: 2571090]

7. Bone N, Millar JB, Toda T, Armstrong J. Regulated vacuole fusion and fission in Schizosaccharomyces pombe: an osmotic response dependent on MAP kinases. Curr Biol 1998;8:135–144. [PubMed: 9443913]

8. Wang YX, Kauffman EJ, Duex JE, Weisman LS. Fusion of docked membranes requires the armadillo repeat protein Vac8p. J Biol Chem 2001;276:35133–35140. [PubMed: 11441010]

9. Wang L, Seeley ES, Wickner W, Merz AJ. Vacuole fusion at a ring of vertex docking sites leaves membrane fragments within the organelle. Cell 2002;108:357–369. [PubMed: 11853670]

10. Roberts CJ, Raymond CK, Yamashiro CT, Stevens TH. Methods for studying the yeast vacuole. Methods Enzymol 1991;194:644–661. [PubMed: 1706462]

11. LaGrassa TJ, Ungermann C. The vacuolar kinase Yck3 maintains organelle fragmentation by regulating the HOPS tethering complex. J Cell Biol 2005;168:401–414. [PubMed: 15684030]

12. Hounsa CG, Brandt EV, Thevelein J, Hohmann S, Prior BA. Role of trehalose in survival of Saccharomyces cerevisiae under osmotic stress. Microbiology 1998;144:671–680. [PubMed: 9534237]

13. Ellis RJ. Macromolecular crowding: obvious but underappreciated. Trends Biochem Sci 2001;26:597–604. [PubMed: 11590012]

14. Parsegian VA, Rand RP, Rau DC. Macromolecules and water: probing with osmotic stress. Methods Enzymol 1995;259:43–94. [PubMed: 8538466]

15. Mayer A, Wickner W, Haas A. Sec18p (NSF)-driven release of Sec17p (a-SNAP) can precede docking and fusion of yeast vacuoles. Cell 1996;85:83–94. [PubMed: 8620540]

16. Sollner T, Bennett MK, Whiteheart SW, Scheller RH, Rothman JE. A protein assembly-disassembly pathway in vitro that may correspond to sequential steps of synaptic vesicle docking, activation, and fusion. Cell 1993;75:409–418. [PubMed: 8221884]

17. Fratti RA, Jun Y, Merz AJ, Margolis N, Wickner W. Interdependent assembly of specific regulatory lipids and membrane fusion proteins into the vertex ring domain of docked vacuoles. J Cell Biol 2004;167:1087–1098. [PubMed: 15611334]

18. Merz AJ, Wickner WT. Resolution of organelle docking and fusion kinetics in a cell-free assay. Proc Natl Acad Sci U S A 2004;101:11548–11553. [PubMed: 15286284]

19. Eitzen G, Will E, Gallwitz D, Haas A, Wickner W. Sequential action of two GTPases to promote vacuole docking and fusion. EMBO J 2000;19:6713–6720. [PubMed: 11118206]

20. Seals DF, Eitzen G, Margolis N, Wickner WT, Price A. A Ypt/Rab effector complex containing the Sec1 homolog Vps33p is required for homotypic vacuole fusion. Proc Natl Acad Sci U S A 2000;97:9402–9407. [PubMed: 10944212]

21. Merz AJ, Wickner WT. Trans-SNARE interactions elicit Ca2+ efflux from the yeast vacuole lumen. J Cell Biol 2004;164:195–206. [PubMed: 14734531]

22. Thorngren N, Collins KM, Fratti RA, Wickner W, Merz AJ. A soluble SNARE drives rapid docking, bypassing ATP and Sec17/18p for vacuole fusion. Embo J 2004;23:2765–2776. [PubMed: 15241469]

23. Boeddinghaus C, Merz AJ, Laage R, Ungermann C. A cycle of Vam7p release from and PtdIns 3-P-dependent rebinding to the yeast vacuole is required for homotypic vacuole fusion. J Cell Biol 2002;157:79–89. [PubMed: 11916982]

24. Starai VJ, Jun Y, Wickner W. Excess vacuolar SNAREs drive lysis and Rab bypass fusion. Proc Natl Acad Sci U S A. 2007

25. Luke CJ, Pak SC, Askew YS, Naviglia TL, Askew DJ, Nobar SM, Vetica AC, Long OS, Watkins SC, Stolz DB, et al. An intracellular serpin regulates necrosis by inhibiting the induction and sequelae of lysosomal injury. Cell 2007;130:1108–1119. [PubMed: 17889653]

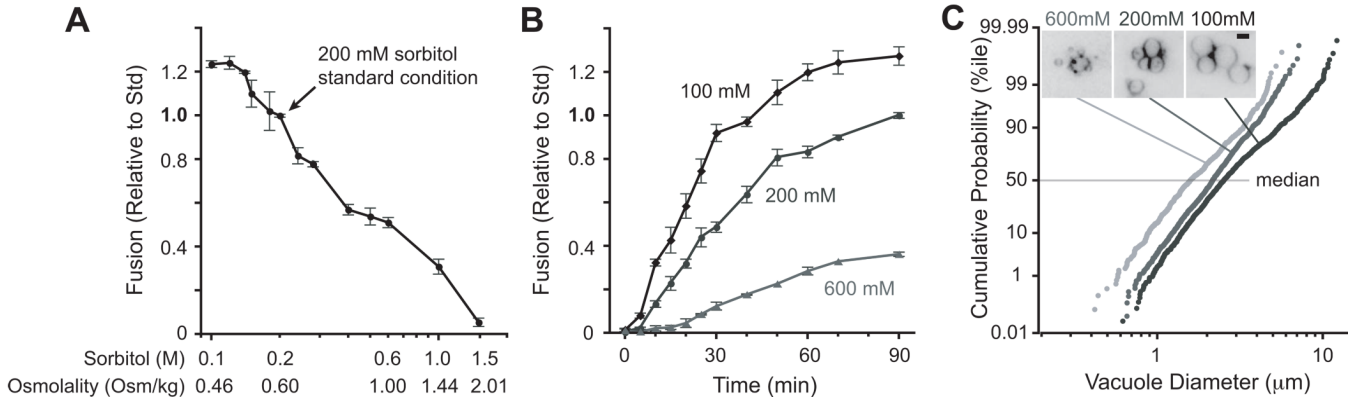26. Haas A. A quantitative assay to measure homotypic vacuole fusion. Meth Cell Sci 1995;17:283–294.

A

B

C

Figure 1. Osmotic control of homotypic vacuole fusion

(A) *In vitro* homotypic vacuole fusion at the indicated concentrations of sorbitol was measured after a 90 min. incubation. On the horizontal axis, measured buffer osmolality is shown for reaction buffers containing the indicated concentrations of sorbitol. n≥4 for each point. **(B)** Kinetics of fusion in hypotonic (100 mM), standard (200 mM), and hypertonic (600 mM sorbitol) conditions. n ≥ 4 for each point; bars span 95% confidence intervals. **(C)** Vacuole diameter increases with fusion. Fusion increases both membrane area and volume, and hence the size of the vacuoles in the population. To crosscheck the results obtained in content mixing assays, vacuole diameter was measured at the end of 70 min. fusion reactions containing the indicated concentrations of sorbitol. The morphometric data are plotted in rank order in cumulative probability histograms., wiht the median vacuole diameter (50th %ile) for each treatment indicated. 500–1000 vacuoles from at least two experiments were measured for each condition. (Inset) Examples of morphology of FM4-64-stained vacuoles after 70 min. incubation with ATP. Scale bar = 2.5 µm.
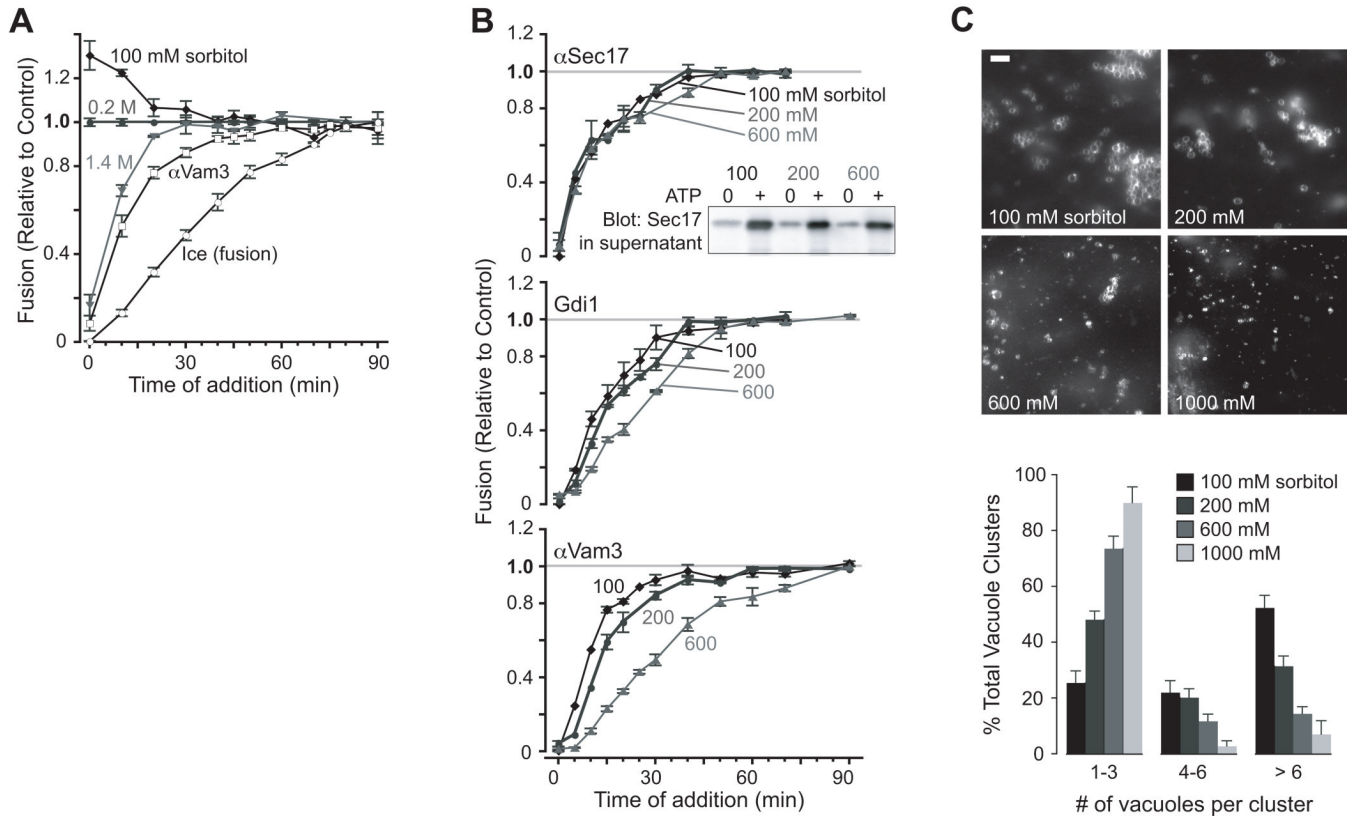
Figure 2. Osmotic control of early docking subreactions
(A) Kinetic mapping of osmotic effect. At the times indicated, aliquots of standard vacuole fusion reactions (200 mM sorbitol) were shifted to a final sorbitol concentration of 100, 200 or 1400 mM, as indicated, and incubated for a total of 90 min. Data are normalized to the values obtained with reactions diluted in isotonic (200 mM sorbitol) buffer. Kinetics are also shown for inhibitors of docking (αVam3p antibody, 35 nM) and fusion (ice) at standard 200 mM sorbitol. n ≥ 4 independent experiments. **(B)** Osmotic control of docking kinetics. At the indicated times, subreaction inhibitors were added to reactions containing 100, 200 or 600 mM sorbitol throughout the incubation. Fusion inhibitors include (from early to late stage inhibition): 322 nM αSec17 antibody; 14 µM rGdi1; 35 nM αVam3 antibody. The data are normalized to fusion values obtained when fusion buffer was added in place of inhibitor at the indicated times (grey lines). (Inset) Vacuoles were incubated with or without ATP for 10 min. in the presence of 100, 200 or 600 mM sorbitol, then sedimented. The amount of Sec17 released from the membrane pellet was determined by western blot analysis using $1/6^{th}$ of the supernatant from each fusion reaction. n ≥ 4 independent experiments. **(C)** Osmotic inhibition of tethering. Images of FM4-64 stained vacuoles after 30 min. of incubation with or without ATP in the presence of 100, 200, 600 or 1000 mM sorbitol. Scale bar = 6 µm. Vacuole clusters were scored under each condition, and data is presented as a percentage of total. A cluster refers to a single group of vacuoles. At least 200 clusters were counted for each condition.
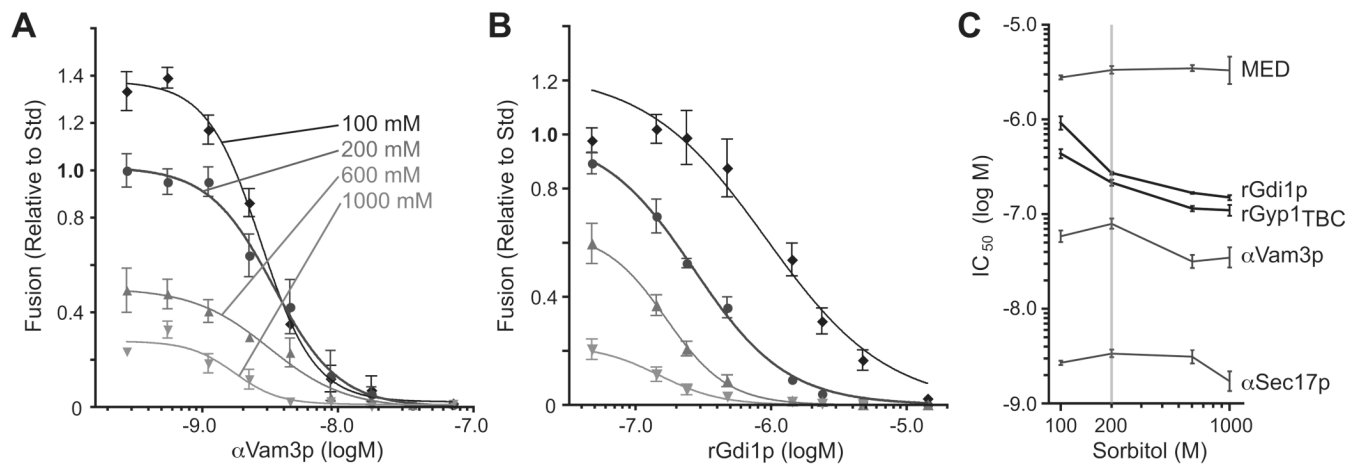
Figure 3. Osmolytes enhance sensitivity of fusion to Rab inhibitors
Homotypic vacuole fusion was measured after vacuoles were incubated with ATP for 90 min. in the presence of 100, 200, 600 or 1000 mM sorbitol and increasing concentrations of **(A)** anti-Vam3 antibody or **(B)** rGdi1p. Sigmoidal dose-response curves were fit to the datasets. **(C)** IC_{50} values were extracted from the fits shown in A and B, and from similar curves for other inhibitors (see Fig. S3A–C). Bars span 95% confidence intervals; n ≥ 4 for all experiments shown. Dose-response for additional inhibitors and an alternative presentation of the IC_{50} values is presented in Fig. S3D.
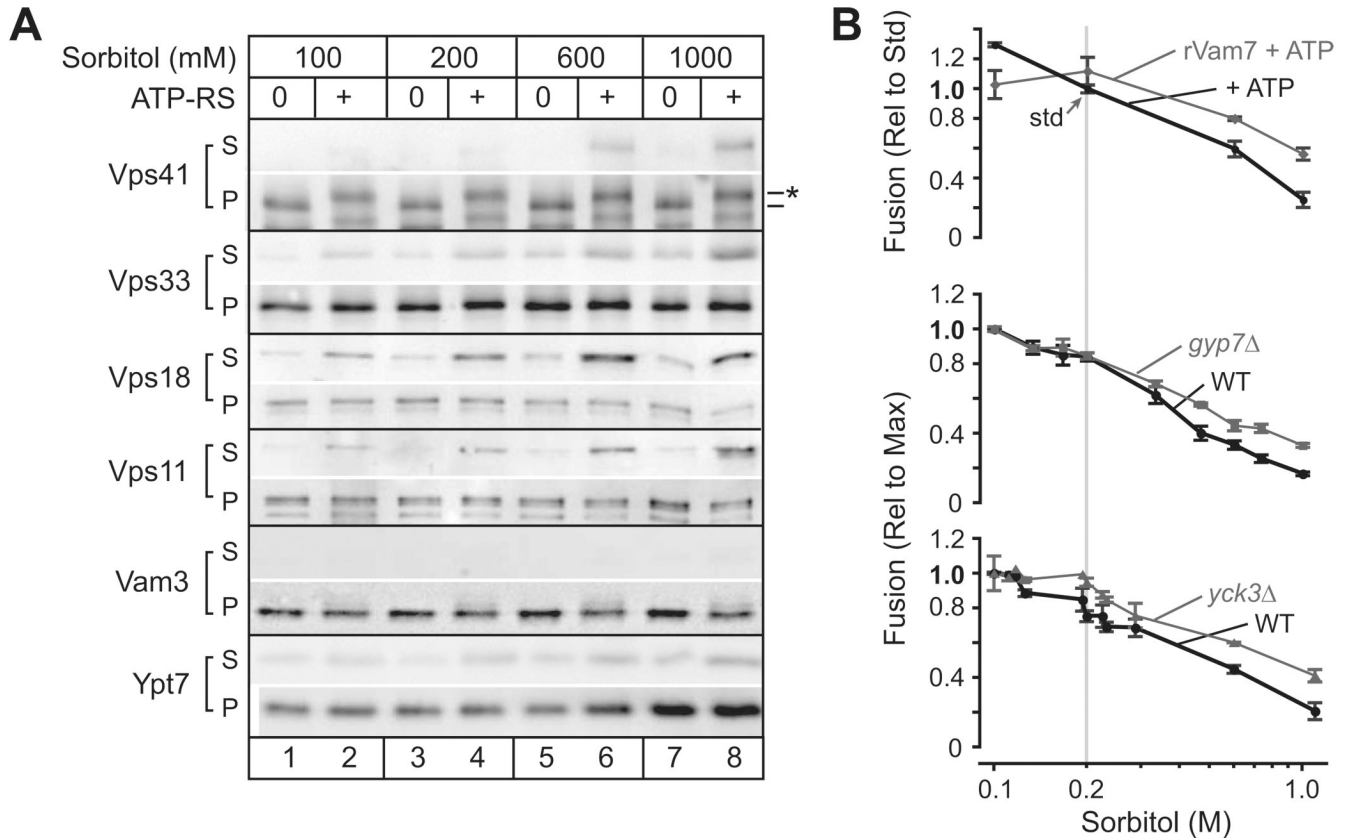
Figure 4. Interplay between osmotic strength and docking factors
(A) Osmolyte-triggered HOPS dissociation from the vacuole. Vacuoles were incubated with or without ATP for 70 min. in the presence of 100, 200, 600 or 1000 mM sorbitol, then sedimented. Membrane association of 4 HOPS components (Vps41, Vps33, Vps18 and Vps11), a vacuole Q_a-SNARE (Vam3), and the vacuole Rab GTPase (Ypt7) was assessed by western blot using 1/3 of the total isolated supernatent (S) and 1/10 (0.6 μg vacuole protein) of the pellet (P). Phospho-Vps41 (*) was observed exclusively in the presence of ATP, as reported [11]. **(B)** Rab activation or partial Rab bypass attenuates inhibition by osmolyte. Top: Vacuoles were incubated for 90 min. with ATP at increasing sorbitol concentrations in the the presence and absence of recombinant Q_c-SNARE rVam7, which reduces the Ypt7 requirement in fusion [21,22], Middle, bottom: vacuoles were purified from yeast strains containing or lacking Gyp7 (middle), which when absent stabilizes membrane association of Ypt7 and components of HOPS (inset B; Fig. 4S), or the vacuolar casein kinase I Yck3 (bottom), which, when absent, stabilizes HOPS on the membrane [11]. Fusion data were normalized to either the mean rate of fusion under standard conditions (ATP only, 200 mM sorbitol; top) or conditions where maximum fusion values were observed (100 mM sorbitol; middle, bottom). n ≥ 4 for each point.